Journal of Environmental Management 349 (2024) 119501

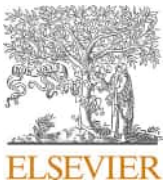

Contents lists available at ScienceDirect

Journal of Environmental Management

journal homepage: www.elsevier.com/locate/jenvman

Research article

Valorization of lead-zinc mine tailing waste through geopolymerization: Synthesis, mechanical, and microstructural properties

Dawei Li, Andrea O. Ramos, Alseny Bah, Feihu Li *

Collaborative Innovation Centre of Atmospheric Environment and Equipment Technology, Jiangsu Key Laboratory of Atmospheric Environment Monitoring and Pollution Control, School of Environmental Science and Engineering, Nanjing University of Information Science and Technology, 219 Ningliu Road, Nanjing 210044, China

ARTICLE INFO

Keywords:
Geopolymer
Solidification
fly ash
Mine tailings
Mechanical strength
Microstructure

ABSTRACT

Lead-zinc mine tailing waste can have significant environmental impacts due to its potential for releasing toxic elements into the surroundings and contaminating local soil and water. This paper focuses on the valorization of lead-zinc mine tailing waste through geopolymerization, a sustainable process that can transform waste into useful building materials. Geopolymer matrixes with various mixtures of mine tailing (0−100 wt%), fly ash (0−100 wt%), and flue gas desulfurization (FGD) gypsum (0, 5, and 10 wt%) were synthesized using different activators such as sodium hydroxide (NaOH, 5, 10 M) and sodium silicate (waterglass, 0, 12.5 wt%). Visual inspection, unconfined compressive strength (UCS) testing, and microstructural analysis (e.g., X-ray diffractions, Fourier transforms infrared, and scanning electron microscopy) were employed for the physicochemical characterization of these geopolymers. The highest UCS value of 24.1 MPa was observed in a geopolymer specimen with 100 wt% fly ash and activated by 10 M NaOH and cured for 28 days. The blending of mine tailings would result in strength recession, e.g., the integrating of 25 wt% tailings showed a UCS of 12.3 MPa. The addition of 5 wt% gypsums can improve early strength development, particularly for matrixes with 50–75 wt% fly ash. But adding 10 wt% gypsums would lead to strength retrogression of the resulting geopolymers. The introduction of waterglass can also facilitate geopolymerization and improve strength development. However, the cointegrating of gypsum and waterglass can induce an antagonistic effect and lead to the collapse of the geopolymer specimens. The findings revealed that the strength and microstructural properties of geopolymer are determined by the matrix compositions, alkaline activators, etc. Effective regulation of these factors can produce geopolymer matrixes with high dimensional stability and UCS that well meet construction material standards. Overall, the study indicates that geopolymerization represents a viable and eco-friendly solution for valorizing lead-zinc mine tailing waste and gaining alternative building materials.

1. Introduction

Mining and mineral processing activities around the world generate millions of metric tons of mine tailings (MTs) annually, which poses an increasing and lasting threat to local environments, in particular the soil and groundwater systems, and thereby the surrounding ecosystems (Alvarez-Ayuso, 2022; Park et al., 2019). Tailing wastes from lead-zinc mining and/or mineral processing, for example, often contain high levels of hazardous elements such as lead (Pb), copper (Cu), arsenic (As), chromium (Cr), zinc (Zn), etc. (Bah et al., 2022b; Li et al., 2016b; Xia et al., 2019), thus creating significant environmental and health risks if stored or disposed of improperly. Moreover, the safe storage and proper handling of these tailing wastes are costly and land-intensive, which will place an additional financial burden on local governments, especially those in developing countries.

Value-added utilization or valorization of such MTs through geopolymerization to meet the expanding needs of the construction industry is, however, a promising and sustainable approach to address these challenges (Ahmari and Zhang, 2013). Indeed, the majority of the chemical components in such tailing wastes are primarily composed of silicon (Si), aluminum (Al), calcium (Ca), iron (Fe), and manganese (Mn) oxides, accounting for about 60–90% of the total mass (Bah et al., 2022a; He et al., 2022; Wang et al., 2023). Once activated with alkali, these oxides would yield inorganic polymeric cementitious substances similar to those found in ordinary Portland cement (OPC) mortars (Duxson et al., 2007). This process is known as geopolymerization (Duxson et al.,

* Corresponding author.
E-mail address: fhli@nuist.edu.cn (F. Li).

https://doi.org/10.1016/j.jenvman.2023.119501
Received 7 June 2023; Received in revised form 10 October 2023; Accepted 26 October 2023

2007). As long as the mechanical strength and leachate of the resulting geopolymer specimens meet the relevant standards for specific construction materials, they can therefore be used as alternatives to such materials (Zhang et al., 2021c). Benefiting from their high enough mechanical strength, physical integrity, and lower CO_2 emissions compared to OPC mortars, these MT-base geopolymers have been widely used in a variety of industrial scenarios (Li et al., 2012; Majidi, 2009; Rao and Liu, 2015), including construction binders or concretes (Mabroum et al., 2020; Nguyen et al., 2023; Zhang et al., 2021b), road base construction (Manjarrez et al., 2019; Manjarrez and Zhang, 2018), paste backfills (Behera et al., 2020; Jiang et al., 2019; Ouffa et al., 2022), solidification/stabilization (S/S) (Kiventera et al., 2018; Opiso et al., 2021; Wang et al., 2023; Zhang et al., 2020), adsorbents (Aouan et al., 2023; Nguyen et al., 2023), etc.

To improve the overall quality, in particular, the mechanical strength of MT-based geopolymers, fly ash (FA), and other industrial byproducts (e.g., flue gas desulfurization (FGD) gypsum, cement kiln dust, aluminum sludge, etc.) are often incorporated concurrently into the parent material mixture when preparing such geopolymers (Ahmari and Zhang, 2013; Ren et al., 2015; Zhang et al., 2022). Including class F fly ash into MT mixtures, for instance, not only improved the geopolymerization effects but also significantly enhanced the compressive strength of MT-based geopolymer by 82.2% in the case of incorporating 15% of FA (Zhang et al., 2022). Introducing gypsum into Pb–Zn smelting wastes can increase the mechanical strength of the resulting geopolymers, but the excessive blending of gypsum (>12%) would lower their immobilization performance towards toxic elements, in particular, arsenic (Li et al., 2016b). Our previous study also demonstrates that the addition of both FA and FGD gypsum to Pb–Zn MTs can simultaneously improve the unconfined compressive strength (UCS) of the geopolymer specimens and their immobilization performance for exogenous arsenic, apart from the endogenous toxins in such Pb–Zn tailings (Bah et al., 2022b). Several studies have extensively explored the physicochemical properties, and preparation aspects of Pb–Zn MT-based geopolymers (Krishna et al., 2021; Lazorenko et al., 2021; Zhang et al., 2021a), nonetheless, the influences of many factors (e.g., material matrix ratio, activator, etc.) on both the mechanical and the microstructural properties of such geopolymers remain limitedly understood.

This work aims to evaluate the feasibility of valorization of Pb–Zn mine tailings through alkali-activated geopolymerization with sodium hydroxide and/or a mixture of sodium hydroxide and sodium silicate as the activator, and class F fly ash and FGD gypsum as the additive. The effects of material ratio, alkaline concentration, and curing time on the mechanical strength of geopolymer specimens were comprehensively evaluated through unconfined compressive strength tests. Besides, the microstructural analysis of pulverized geopolymer specimens was performed by using X-ray diffraction (XRD), Fourier-transform infrared spectroscopy (FTIR), and scanning electron microscopy (SEM). This work is presented an alternative approach for valorizing Pb–Zn mine tailings by geopolymerization, and highlights rational manipulating of these factors, in particular the material matrix ratio, can yield geopolymer products with superior dimensional stability and high compressive strength that well meet construction material criteria.

2. Materials and methods

2.1. Materials

Sodium hydroxide (NaOH, ≥96%) was purchased from Macklin Biochemical Co., Ltd. (Shanghai, China) and used as the activator. Another activator — Sodium silicate solution (waterglass, SiO_2 13.36%, Na_2O 29.84%) was obtained from Ganjiashan Yourui Refractories Co., Ltd. All chemicals were used as received without further purification. Distilled water was used to prepare solutions for geopolymer synthesis. Class F fly ash (FA), and FGD gypsum (Gp) were obtained from Jiangsu Nanre Power Generation Co., Ltd. (Nanjing, China), whereas the Pb–Zn mine tailings (MT) were gained from Nanjing Yinmao Pb–Zn Mining Industry Co., Ltd. (Nanjing, China). The chemical compositions and trace elements of both FA and MT have been determined and discussed in our earlier study (Bah et al., 2022b). The mineralogical, elemental compositions, and morphological properties of these raw materials are briefly depicted in Fig. 1.

2.2. Synthesis of geopolymer

As illustrated in Fig. 2a, geopolymer specimens were prepared following our previous study (Bah et al., 2022b). Briefly, a certain amount of raw material powders was dry mixed for 10 min to achieve homogenization, followed by gradually adding the alkaline liquid such as NaOH solution (5 or 10 M) or a mixture of waterglass and NaOH (mass ratio = 1.08:1) and further blending for 15 min. For instance, blending 200 g of fly ash with 54 g of NaOH solution (5 M) can make a paste for geopolymer with only fly ash as the raw material. The sodium hydroxide solution was prepared by dissolving 40 g of NaOH flakes into distilled water in a plastic beaker. Then the solution was air-cooled and its total volume was adjusted to 200 or 100 mL to yield a 5 or 10 M NaOH solution. To avoid the influence of exogenous heat from the dissolution of NaOH on the alkali activation reactions, the as-prepared NaOH solution was sealed and cooled down to ambient temperature before further utilization. The resulting homogeneous pastes were then cast into six-fold concrete cube test steel molds ($20 \times 20 \times 20$ mm^3) at ambient temperature, followed by curing for 72 h before demolding. The geopolymer specimens were covered with a polyethylene film in a lab tray and cured at ambient temperature (~25 °C) for 7, 14, and 28 days. All geopolymer specimens were prepared in triplicate. The geopolymer specimen composition matrix is tabulated in Table 1, where each specimen was encoded with the initials of its raw materials, e.g., a specimen with code of FGMSW means the geopolymer was prepared by using a mixture of fly ash, mine tailing, gypsum, sodium hydroxide, and waterglass (F – fly ash, M – mine tailings, G – gypsum, S – sodium hydroxide, W – waterglass). Since the leachability of toxic elements of concern was far below the Chinese standard levels after geopolymerization (Bah et al., 2022b), the leachability of such elements was not evaluated in this study.

2.3. Mechanical strength testing

The unconfined compressive strength (UCS) testing was employed to evaluate the air-cured geopolymers' solidification effectiveness following the protocol specified by the ASTM C109/C109M-08 standard (ASTM Standard C109/C109M-08, 2009). The effects of NaOH concentration, contents of FA, Gp, and waterglass, and curing time on the mechanical strength of the geopolymer specimens were studied systematically. In brief, the geopolymer specimens after 7-, 14-, and 28-day curing were measured on a WDW-100 universal material testing apparatus (Jinan Fangyuan Test Instrument Co., Ltd., China) at a constant loading of 5 MPa s^{-1}. Once the geopolymer specimen began to crack, the machine stopped automatically and the corresponding applied force value (in kN) was obtained. Then the UCS value can be attained by dividing the applied force by the corresponding area of action (i.e., 20×20 mm^2). The crushed geopolymer pieces were collected for further microstructural characterization. Each geopolymer specimen was tested in triplicate and the average UCS value and its standard deviation (SD) were attained for further analysis.

2.4. Microstructural analysis

To explore the microstructural features of geopolymer contributing to its mechanical strength and bulk integrity, the crushed geopolymer specimens were then pulverized for further characterizations as used for their raw materials. Specifically, X-ray diffraction (XRD) analysis was performed on an XRD-6100 diffractometer (Shimadzu, Japan) at a tube

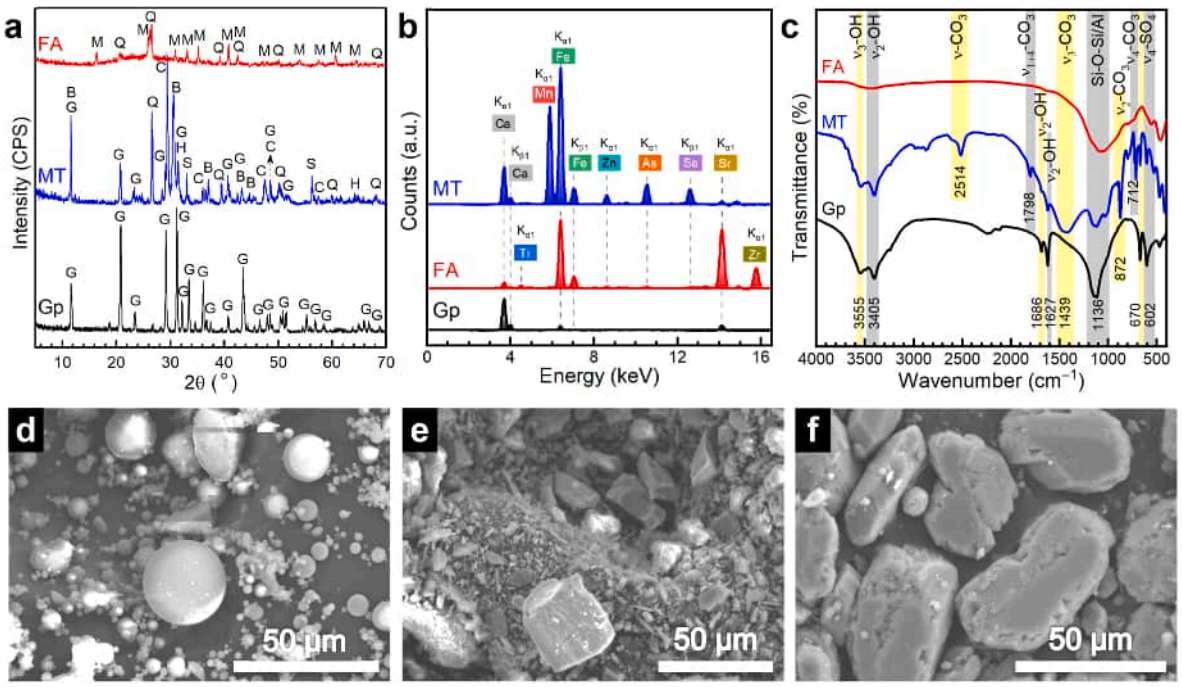

Fig. 1. Characterizations of the three raw materials — fly ash (FA), mine tailing (MT), and flue gas desulfurization (FGD) gypsum (Gp). (**a**) XRD patterns, (**b**) XRF spectra, (**c**) FTIR spectra; (**d**–**f**) SEM images of (**d**) fly ash, (**e**) mine tailing, and (**f**) gypsum. Notations in panel (**a**): B – Brushite (JCPDS #09–0077), C – Calcite (JCPDS #05–0586), G – Gypsum (JCPDS #33–0311), H – Gehlenite (JCPDS #35–0755), M – Mullite (JCPDS #15–0776), Q – Quartz (JCPDS #46–1045), S – Sphalerite (JCPDS #05–0566).

voltage of 40 kV and a tube current of 30 mA with Cu-Kα radiation (step size: 0.02°, scanning rate: 5° min^{-1}). X-ray fluorescence spectroscopy (XRF) analysis of the raw materials was conducted on a portable DELTA DC 4000 analyzer (Olympus, USA) with soil mode. Fourier Transform Infrared Spectroscopy (FTIR) data were collected on Is5 infrared spectrometer (Thermo Nicolet, USA) following the KBr pellet method. Scanning electron microscopy (SEM) was also used for the morphological investigation of several selected geopolymer specimens on a SU1510 microscope (Hitachi, Japan).

3. Results and discussion

3.1. Characterization of raw materials

The mineral components of FA, MT, and Gp determined by XRD are shown in Fig. 1a. Using the Whole Pattern Fitting (WPF) module within Jade 6.5 software (Materials Data, Inc., USA), the mineral component of FA was calculated to be 67.6% of amorphous phase, 24.5% of mullite (JCPDS #15–0776), and 7.9% of quartz (JCPDS #46–1045) (Bah et al., 2022a). Note that MT is mainly consisted of calcite (JCPDS #05–0586), quartz, brushite (JCPDS #09–0077), gypsum (JCPDS #33–0311), and minor gehlenite (JCPDS #35–0755), and sphalerite (JCPDS #05–0566), whereas Gp is essentially comprised of high purity gypsum. The surface element compositions of all these raw materials (Fig. 1b) are in good consistence with the above XRD data, even though some metals cannot be detected due to the limitation of the portable XRF apparatus (Olympus, 2013). In addition, apart from the vibrations of water molecules over 1627–3555 cm^{-1} and the stretching of Si–O–Si/Al groups at 1136 cm^{-1} in the FTIR spectra of these raw materials (Bah et al., 2022b), the blending vibration of sulfate group (ν_4-SO_4) at 602 cm^{-1} was also observed for both MT and Gp, indicative of the existence of gypsum, which is consistent with the above XRD results. Moreover, note that the spectrum of MT is characterized by bands at 2514, 1798, 872, and 712 cm^{-1} assignable to stretching and/or blending vibrations of carbonate (ν-CO_3) (Prasad, 2005), confirming calcite is a major component of MT as evidenced by XRD analysis (see Fig. 1a).

The morphologies of these raw materials are depicted in Fig. 1d–f. FA is featured by smooth spheres (cenospheres) ranging from 2 to 30 μm, which is very similar to other typical class F fly ash as observed elsewhere (Li et al., 2016a). Gp is composed of kidney bean-like particles with a size of 10–50 μm, whereas MT consists of a large number of irregular particles with diverse size distribution. The unique morphological characteristics of these particles are beneficial for the identification of unreacted or partially reacted particles and the interpretation of the gelation process inside the geopolymer material after alkali activation (Bah et al., 2022b; Ken et al., 2015).

Furthermore, the geopolymerization and/or reactivity of these geopolymer precursors is also determined by their chemical compositions which were already tabulated in our earlier paper (Bah et al., 2022a). The two major compositions in FA, for example, are amorphous SiO_2 and Al_2O_3, accounting for 40.15% and 35.5% of the total mass, respectively. In the case of MT, however, CaO and SiO_2 are the predominant components, contributing 29.49% and 18.83%, respectively (Bah et al., 2022a). All these metal oxides are the essential components in the formation of calcium silicate hydrate (C–S–H) and calcium aluminate silicate hydrate (C-A-S-H) during the geopolymerization process (Li et al., 2007, 2012).

3.2. Dimensional stability of bulk geopolymer cubes

From the perspective of practical applications, the dimensional stability of any cementitious binders including geopolymers, is crucial for their use in a real engineering scenario, since concretes and other building blocks are obliged to neither shrink nor expand excessively in service (Shi et al., 2019). Maintaining the dimensional stability of MT-based geopolymers is thus a significant challenge for valorizing MT wastes while also meeting the requirements of stringent building material standards. In general, geopolymers with superior mechanical strength often demonstrate higher dimensional stability in comparison to their counterparts with inferior mechanical properties (Ken et al.,

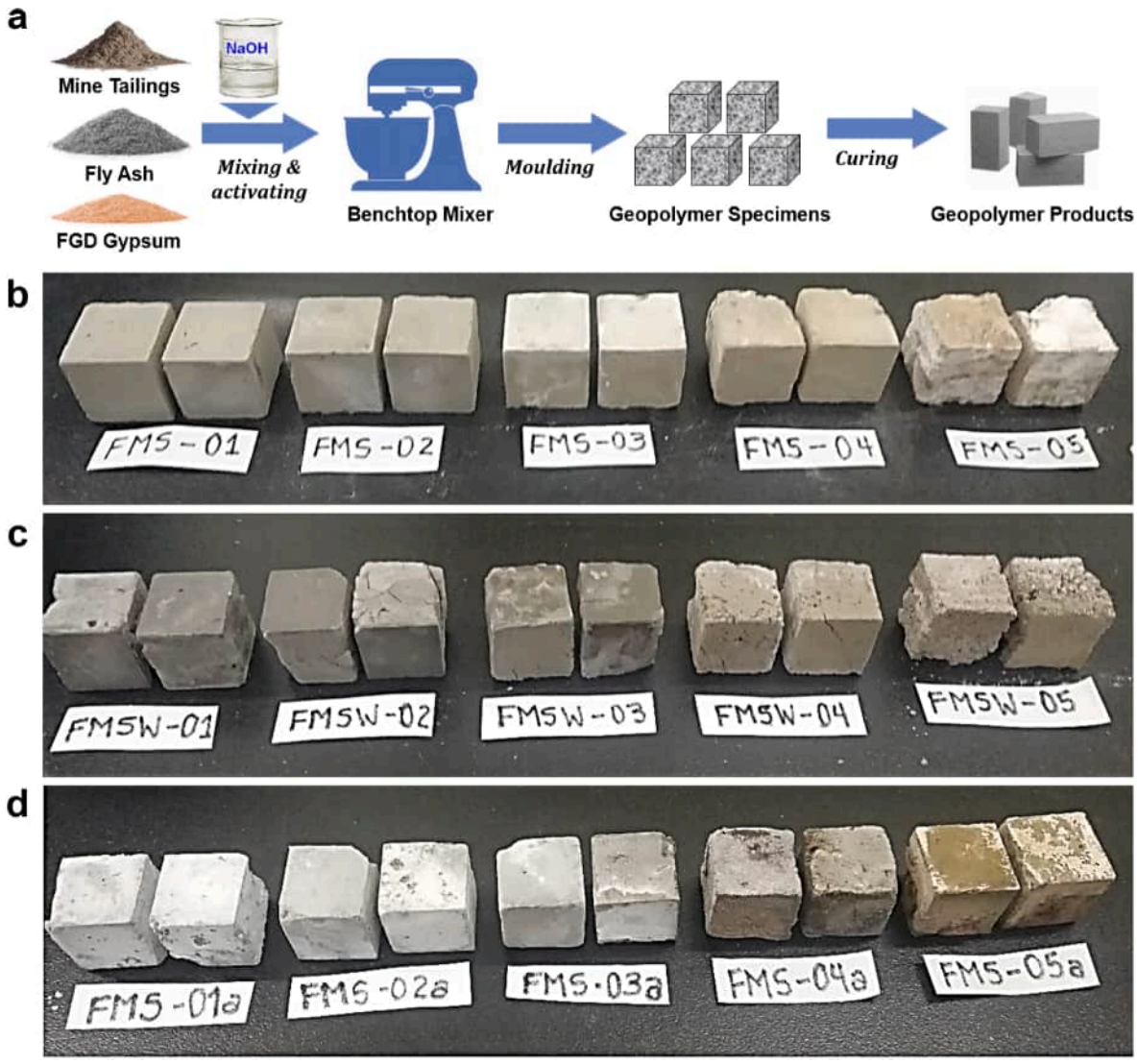

Fig. 2. (**a**) Schematic illustration of the geopolymer preparation procedure; (**b**–**d**) Visual inspections (digital images) of the as-prepared geopolymer cubes, (**b**) fly ash-mine tailing-sodium hydroxide (FMS) series, (**c**) fly ash-mine tailing-sodium hydroxide-waterglass (FMSW) series, and (**d**) fly ash-mine tailing-sodium hydroxide (10 M) (FMS-a) series after curing for 28 days.

2015). The dimensional stability can, therefore, be used as an initial visual indicator for assessing the mechanical property of geopolymer specimens. In the present study, visual inspection was adopted as an initial screening tool before more advanced testing (e.g., UCS testing, XRD) for evaluating the dimensional integrity of geopolymer specimens. By visually examining the surface of the specimen, one can identify any visible cracks or deformations that may have occurred during the casting, curing, or manufacturing process.

The digital images of each series of geopolymer specimens after curing for 28 days are shown in Fig. 2b–d, and S1–2 (Supplementary Information). A visual examination of the FMS series specimens (Fig. 2b) indicated that surface deterioration or corner collapse appears to occur as the FA content decreased from 100% to 0. In other words, their dimensional integrity decreases apparently with decreasing FA content. This trend is also true for other series of geopolymers and is attributed to the very high content of active silica and alumina in FA, which can generate silicate gels with high connectivity upon NaOH activation, thereby leading to excellent dimensional stability (Provis and Bernal, 2014). Note that the introduction of WG to the above series of geopolymers appears to result in a moderate decline in dimensional stability (*cf*. Fig. 2b and c). This is due to the relatively low connectivity of silanol groups inside the geopolymers when using a silicate (e.g., waterglass) as the activator (Provis et al., 2009). A higher level of NaOH as the activator is often beneficial to the gelation of silica-aluminum oxides and thus their strength development as well as dimensional integrity. This is evidenced by the visual inspection of the FMS-a series geopolymers with 10 M NaOH as an activator compared to the FMS series specimens with 5 M NaOH (*cf*. Fig. 2b and d). Interestingly, the FMS-05a specimen is covered by a green mineral after 28-d curing, which is likely to be chabazite derived from the reaction between NaOH and MT with a proper ratio of metal oxides (Bah et al., 2022a).

In addition, the incorporation of 5 wt% of Gp into the FMS series of geopolymers seems not to affect the dimensional stability too much according to visual inspection of the FGMS series of specimens (*cf*. Fig. 2b and Fig. S1a), but the dimensional integrity of FGMS-a series of geopolymers is reduced when the dosage of Gp was raised to 10 wt% (Fig. S1b). This observation indicates that a high dosage of Gp in geopolymers is detrimental to their stability, in good agreement with previous reports (Ken et al., 2015; Li et al., 2016b). Likewise, the introduction of waterglass into the above specimens also demonstrated a harmful effect on the dimensional stability of the FGMSW series geopolymers (see Fig. S2a). Increasing the dosage of Gp from 5 to 10 wt% (i.

Table 1
The geopolymer specimen composition matrix.

Specimen Code	NaOH	Waste materials (g)			Ratios			
		FA	Gp	MT	Si/Al	Na/Al	Liquid/Solid	WG/NaOH
FMS-01	5 M	200	–	0	1.00	0.18	0.27	–
FMS-02		150	–	50	1.15	0.24	0.27	–
FMS-03		100	–	100	1.44	0.35	0.27	–
FMS-04		50	–	150	2.21	0.64	0.27	–
FMS-05		0	–	200	10.33	3.69	0.27	–
FMS-01a	10 M	200	–	0	1.00	0.37	0.27	–
FMS-02a		150	–	50	1.15	0.48	0.27	–
FMS-03a		100	–	100	1.44	0.70	0.27	–
FMS-04a		50	–	150	2.21	1.27	0.27	–
FMS-05a		0	–	200	10.33	7.37	0.27	–
FMSW-01	5 M	200	–	0	1.09	0.52	0.52	1.08:1
FMSW-02		150	–	50	1.27	0.69	0.52	1.08:1
FMSW-03		100	–	100	1.62	1.00	0.52	1.08:1
FMSW-04		50	–	150	2.54	1.82	0.52	1.08:1
FMSW-05		0	–	200	12.25	10.53	0.52	1.08:1
FGMS-01	5 M	200	10	0	1.00	0.18	0.32	–
FGMS-02		150	10	50	1.15	0.24	0.32	–
FGMS-03		100	10	100	1.44	0.35	0.32	–
FGMS-04		50	10	150	2.21	0.64	0.32	–
FGMS-05		0	10	200	10.33	3.69	0.32	–
FGMS-01a	5 M	200	20	0	1.00	0.18	0.37	–
FGMS-02a		150	20	50	1.15	0.24	0.37	–
FGMS-03a		100	20	100	1.44	0.35	0.37	–
FGMS-04a		50	20	150	2.21	0.64	0.37	–
FGMS-05a		0	20	200	10.33	3.69	0.37	–
FGMSW-01	5 M	200	10	0	1.09	0.52	0.57	1.08:1
FGMSW-02		150	10	50	1.27	0.69	0.57	1.08:1
FGMSW-03		100	10	100	1.62	1.00	0.57	1.08:1
FGMSW-04		50	10	150	2.54	1.82	0.57	1.08:1
FGMSW-05		0	10	200	12.25	10.53	0.57	1.08:1
FGMSW-01a	5 M	200	20	0	1.09	0.52	0.62	1.08:1
FGMSW-02a		150	20	50	1.27	0.69	0.62	1.08:1
FGMSW-03a		100	20	100	1.62	1.00	0.62	1.08:1
FGMSW-04a		50	20	150	2.54	1.82	0.62	1.08:1
FGMSW-05a		0	20	200	12.25	10.53	0.62	1.08:1
FGMSW-01b	10 M	200	20	0	1.09	0.71	0.62	1.08:1
FGMSW-02b		150	20	50	1.27	0.93	0.62	1.08:1
FGMSW-03b		100	20	100	1.62	1.34	0.62	1.08:1
FGMSW-04b		50	20	150	2.54	2.46	0.62	1.08:1
FGMSW-05b		0	20	200	12.25	14.22	0.62	1.08:1

e., the FGMSW-a series) seems not to improve their integrity (*cf.* Figs. S2a and S2b), but a higher level of NaOH can compensate for the loss in dimensional integrity caused by incorporation of both Gp and WG, in particular for specimens with high contents of MT, i.e., FGMSW-04b, 05b (see Fig. S2c). This finding can be explained by the fact that the reaction between Gp and NaOH would yield a high amount of calcium hydroxide that often induces rapid setting and high early strength, and thereby superior dimensional stability (Luukkonen et al., 2018; Malviya and Chaudhary, 2006). Higher dimensional stability usually offers the geopolymer specimens a lower permeability (Zhang et al., 2021c), which is beneficial for the immobilization of toxic elements when applied to S/S, thereof leading to less environmental impact on local ecosystems. Nevertheless, the above visual inspections only offer an initial screening and cannot precisely represent the actual mechanical strength of these specimens, further UCS testing is therefore necessary.

3.3. Effect of curing time on UCS

The curing time often plays a crucial role in determining the mechanical and micro-structural properties of the mine tailing-based geopolymers (Zhang et al., 2011). The effect of curing time on the compressive strength of typical geopolymer specimens as a function of FA content is summarized in Fig. 3. When using 5 M NaOH as the activator (Fig. 3a), the UCS value of geopolymer specimens increases slightly with curing time at low FA content (i.e., 25 wt% FA), while it decreases initially and then increases with the curing time at the FA content of 50 wt%. In the cases of higher FA contents (i.e., >50 wt%), however, it increases initially and subsequently decreases with the curing time. This observation indicates that the UCS of FA/MT-based geopolymer is not entirely governed by the curing time, which is unlike OPC materials, in which prolonged curing time often facilitates its strength development (Khale and Chaudhary, 2007; Sheng et al., 2007). Note that the geopolymer matrixes activated by 10 M NaOH, except for the case of geopolymer with only MT (i.e., the "FA-free" specimen), show a distinct trend of increasing strength with curing time (Fig. 3b), implying that only if the majority of active silica-alumina oxides in the parent matrixes are activated by a sufficient amount of NaOH (e.g., 10 M), the resulting geopolymers exhibit a curing time dependency similar to that of the conventional OPC materials. This is well consistent with earlier reports (Bah et al., 2022b; Jiang et al., 2022).

However, when co-activating by 5 M NaOH and WG, the UCS values of such geopolymer matrixes restore a poorly-defined dependence on the curing time (Fig. 3c), but demonstrate an overall improvement compared to their original counterparts activated solely by 5 M NaOH (cf. Fig. 3a and c). This phenomenon is likely attributed to partial activation of the active silica and alumina in the matrixes by the co-activator, yielding geopolymers with slightly low connectivity of silanol groups (Provis et al., 2009). In the case of the FGMS series (Fig. 3d), the introduction of 5 wt% of Gp to the matrixes appears not to restore the curing time dependency to their UCS values, but slightly improve the early strength (i.e., 7-day UCS) of the resulting geopolymers as expected,

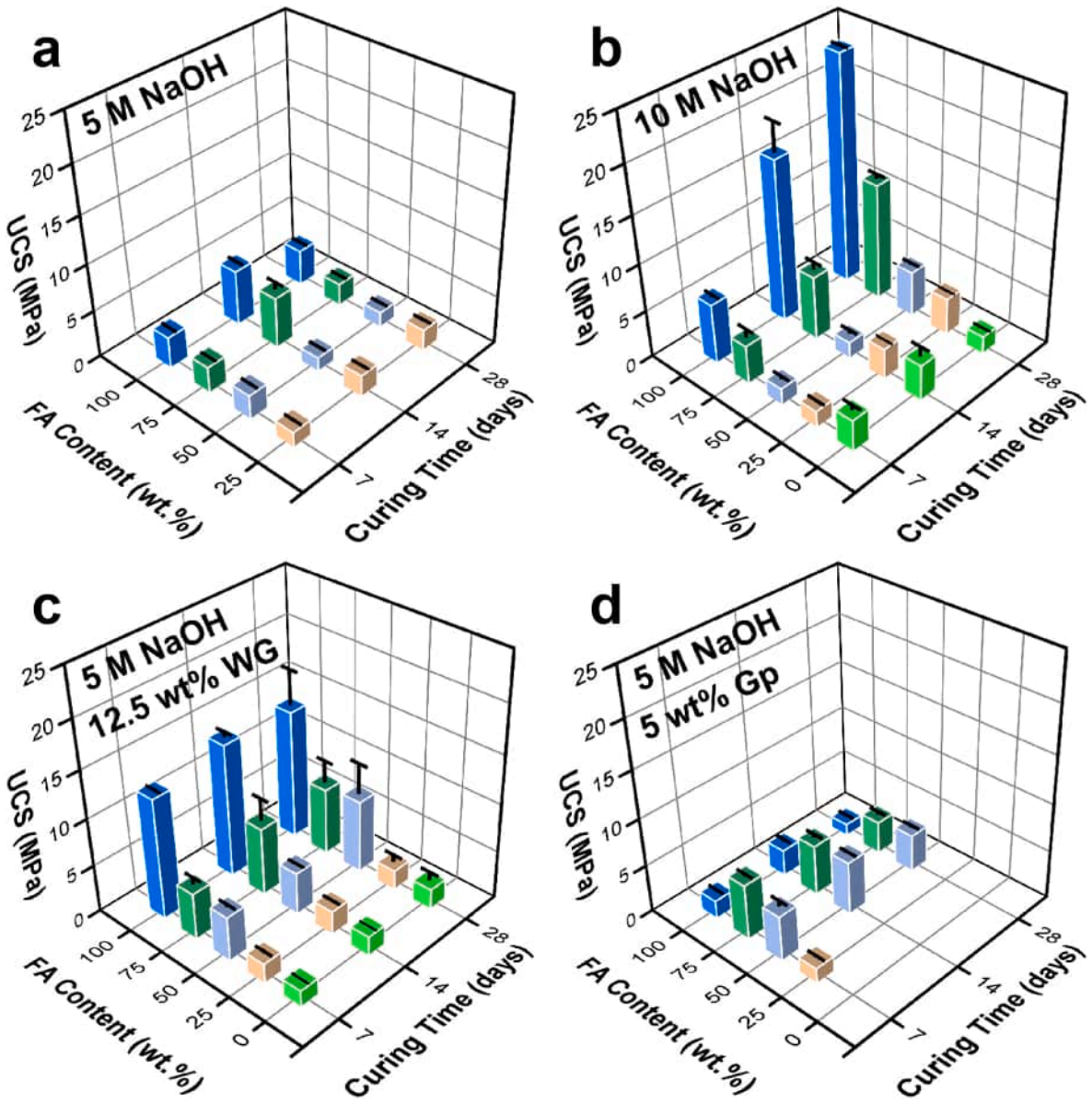

Fig. 3. Effects of curing time and fly ash contents on the UCS of geopolymer specimens using (**a**) 5 M NaOH as the activator (i.e., the FMS (fly ash-mine tailing-sodium hydroxide) series); (**b**) 10 M NaOH as the activator (i.e., the FMS-a (fly ash-mine tailing-sodium hydroxide (10 M)) series); (**c**) 5 M NaOH and 12.5 wt% of waterglass as the activator (i.e., the FMSW (fly ash-mine tailing-sodium hydroxide-waterglass) series); (**d**) 5 M NaOH as the activator with addition of 5 wt% of Gp (i.e., the FGMS (fly ash-gypsum-mine tailing-sodium hydroxide) series).

in particular those with FA content of 50 and 75 wt% (cf. Fig. 3a and d). Briefly, except for the matrixes activated by 10 M NaOH, none of the geopolymer specimens demonstrated a well-defined and unifying dependence between their strength and the curing time. Such poorly-defined dependency between UCS and curing time is often observed in geopolymers incorporated with various types of waste materials (Mohajerani et al., 2019; Singh and Singh, 2019).

3.4. Effects of NaOH and fly ash dosage on UCS

The effect of NaOH molarity on the UCS of geopolymer matrixes as a function of FA content is depicted in Fig. 4a–c and S3 in the Supplementary Information. The UCS values of geopolymer matrixes activated by 10 M NaOH and cured for 7, 14, and 28 days (termed as 7-day, 14-day, and 28-day UCS) are superior to all those activated by 5 M NaOH (Fig. 4a–c). The geopolymer matrix with 100 wt% of FA activated by 10 M NaOH, for example, demonstrates a 28-day UCS as high as 24.1 MPa, over 6 times greater than that of matrix activated by 5 M NaOH (Fig. 4c). In general, a higher NaOH concentration is favorable to the strength development of geopolymers over time (Zhang et al., 2021c). This trend is also evident in this study, particularly for matrixes with FA components and activated by 10 M NaOH (see Fig. 3b and 4a–c). In the case of geopolymers with 10 wt% of Gp and 12.5 wt% of waterglass, matrixes activated by 10 M NaOH also demonstrate a higher UCS than the corresponding counterparts activated by 5 M NaOH and cured for varying periods (Fig. S3), mainly because the more Na^{+} and OH^{-} released from dissociation of NaOH, the faster dissolution of the silica- and alumina-rich phase, and thereby the faster strength development of the resulting geopolymer (Rees et al., 2007).

Likewise, the effect of FA content on the strength properties of geopolymers as a function of NaOH molarity, WG and/or Gp contents are presented in Fig. 4, and S4–5 (Supplementary Information). Note that the matrixes activated by 5 M NaOH show 7-day UCS values increasing linearly with FA content (Fig. 4a), 14-day and 28-day UCS

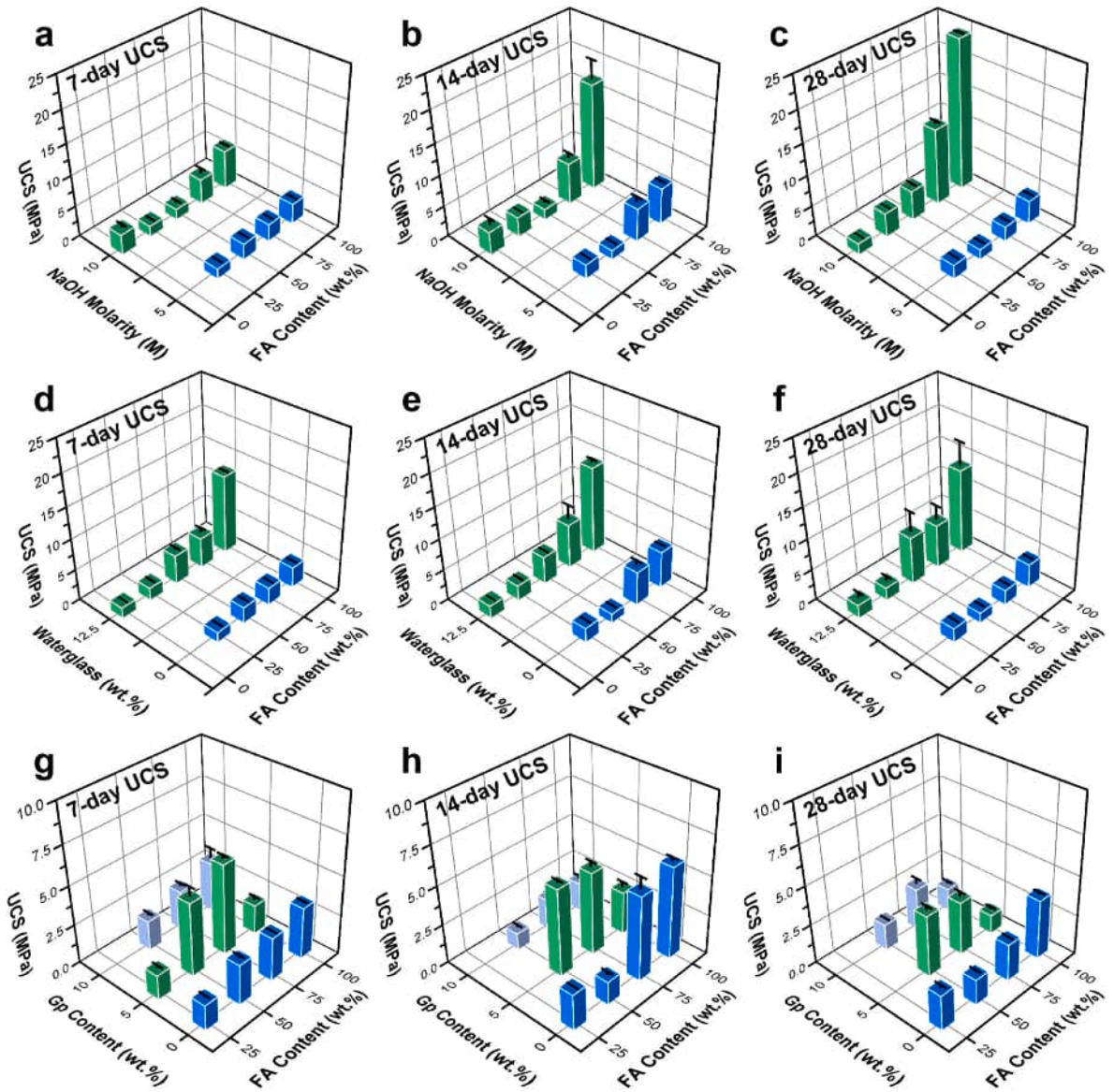

Fig. 4. Effects of NaOH concentration and fly ash (FA) contents on the (**a**) 7-day, (**b**) 14-day, and (**c**) 28-day UCS of geopolymer specimens without the addition of waterglass (i.e., FMS vs FMS-a series); effects of waterglass and FA contents on (**d**) 7-day, (**e**) 14-day, and (**f**) 28-day UCS of geopolymer specimens using 5 M NaOH as the activator (i.e., FMS vs FMSW series); effect of gypsum (Gp) and FA contents on (**g**) 7-day, (**h**) 14-day, and (**i**) 28-day UCS of geopolymer specimens using 5 M NaOH as the activator (i.e., FMS vs FGMS vs FGMS-a series).

with a different FA-dependency (i.e., declining with FA content over the range of 25–50 wt%, but increasing in 50–100 wt%) (Fig. 4b–c). When activating by 10 M NaOH, however, these matrixes demonstrate UCS with varying trends of FA-dependency (Fig. 4a–c). Specifically, both the 7-day and the 14-day UCS decrease with FA content over the range of 0–50 wt% and then increase in 50–100 wt%, but the 28-day UCS values are found to be positively correlated with FA content. As discussed above, it appears that the alkali is sufficient enough for fulfilling the gelation reaction when using 10 M NaOH as the activator for the FMS series of geopolymer matrixes. Moreover, the MT component contains more gypsum and calcite minerals (Fig. 1a) but fewer amorphous phases than FA as indicated previously (Bah et al., 2022b). Given the fact that high calcium material is favorable for yielding a higher early strength to the resulting geopolymers (Ken et al., 2015), it would not be surprising that the early and moderate strength values (7-day, 14-day UCS) of these matrixes decrease slightly with increasing FA content over 0–50 wt% (i.e., decreasing MT content). From an environmental management perspective, a trade-off between the mechanical strength development of the resulting geopolymers and the maximum consumption of MT within the geopolymer matrix should be achieved for a sustainable development.

In the case of matrixes activated by 5 M NaOH and 12.5 wt% of WG (FMSW series), all the UCS values demonstrate a well-defined positive dependent on FA content (Fig. 4d–f). Such dependency was also observed for specimens co-blended with 12.5 wt% of WG and 5 wt%, and 10 wt% of Gp, respectively (Figs. S4 and S5). A possible explanation for this observation is that waterglass can promote the hydrolysis of the siliceous and aluminum species of the raw materials besides offering additional silicate and sodium species required for geopolymerization (Oh et al., 2010).

3.5. *Effect of waterglass and gypsum dosage on UCS*

The effects of WG on the UCS of geopolymers as a function of FA content are given in Fig. 4d–f, and S4–5 (Supplementary Information). As indicated above, the introduction of WG can facilitate the hydrolysis

of both the Si and Al species as well as provide extra Si and Na^+ components, thereby improving the overall compressive strength. These positive effects from WG are verified by the results in Fig. 4d–f, and S4–5. It is noteworthy that the addition of WG demonstrated a higher increase in the early and moderate strength (7-day, 14-day UCS) of the matrixes (Fig. 4d–e) compared to those activated by 10 M NaOH (Fig. 4a–b), however, the increase in the 28-day UCS by WG was smaller than those by 10 M NaOH (cf. Fig. 4c and f). This is because the activation ability of WG is weaker than that of NaOH (Provis et al., 2009), and the relative low connectivity of silanol groups generated by WG activation is unfavorable for the long-term strength development (Dadsetan et al., 2021).

Fig. 4g–i and S6 illustrate the effect of Gp on the UCS of geopolymers as a function of FA content. The addition of 5 wt% of Gp appears to improve the strength of geopolymers with FA content of 50–75 wt% (Fig. 4g–i) while adversely affecting the strength of the "MT-free" matrixes (100 wt% FA) activated by 5 M NaOH. This is in good agreement with that observed elsewhere (Boonserm et al., 2012). When the Gp dosage was increased up to 10 wt%, however, the abatement in the strength of matrixes compared to the original geopolymers. It is believed that sulfate ions in Gp are capable of dissolving Al^{3+} ions from FA while excessive addition of Gp appears to facilitate the formation of the thenardite phase that is likely to suppress the geopolymerization reaction (Ken et al., 2015). This is why the incorporation of 5 wt% of Gp demonstrates distinct enhancement in strength development, while the addition of 10 wt% of Gp shows an adverse effect on the UCS (Fig. 4g–i). However, the addition of both 5 wt% and 10 wt% of Gp demonstrates adverse impacts on the strength development of geopolymer matrixes activated by the mixture of 5 M NaOH and WG (Fig. S6). This observation is likely due to the volume expansion caused by the reaction between calcium hydroxide and calcium aluminate induced by the cointegration of Gp and WG particularly at a higher liquid/solid ratio (0.57, 0.62) (Fernandez-Jimenez et al., 2007; Zhang et al., 2017), which is also confirmed by the above visual inspection results depicted in Fig. S2a–b. Considering that a UCS of 0.35 MPa is appropriate for the physical integrity of solidification/stabilization waste type to withstand standards landfill overburden pressures (Choi et al., 2009), the majority of geopolymer specimens in this study meet the above criteria (see Fig. 3–4, and S3–6), and hence showing a great promise for S/S applications. However, future research and development of these mine tailing-based geopolymers should focus on identifying and controlling potentially toxic releases when applied to S/S.

3.6. Microstructural properties of geopolymer

To establish a link between the microstructural properties and the compressive strength of geopolymers, XRD analysis, SEM images, and FTIR spectra of selected geopolymer specimens were evaluated in detail. These microstructural results are shown in Fig. 5a–c, and S7–14. FTIR analysis is often considered an appropriate method to study the structural evolution of amorphous alumino-silicates exhibiting high heterogeneity. The characteristic infrared bands identified in common geopolymers are summarized in Table S1 in the Supplementary Information. Notably, the geopolymer with the highest UCS (i.e., the FMS-01a series) is featured with similar XRD patterns of strong reflections assignable to minerals such as quartz, mullite, corundum (JCPDS #46–1212), and a diffusion reflection at 2θ of 20–40° that is likely attributed to the amorphous C–S–H gels (Fig. 5a). The FTIR spectra show a typical band at 1070 cm^{-1}, indicating the presence of stretching vibration of Si–O–Si and/or Si–O–Al groups (Fig. 5b). Note that the above band shifted to lower wavenumber region in the FMS-01a specimens, implying the formation of Si–O–Al groups and thereby the amorphous geopolymer gel (i.e., C–S–H, C-A-S-H) after activation of FA by NaOH (Provis and Bernal, 2014; Zhang et al., 2021b). The geopolymer gels are compact and irregular-shaped agglomerates (see Fig. 5c), which appears to be the root reason for their high compressive strength (Rees et al., 2007). This geopolymerization process is usually perceived as following a process of dissolution of parent materials, formation of oligomers, and subsequent cross-linking of such oligomers into a geopolymer network (Fig. 5d).

Notably, lowering either the FA content of the matrixes (Fig. S7) or the molarity of NaOH (Fig. S8) would definitely result in partial geopolymerization (Figs. S8 and S11) due to the lack of amorphous silica or alumina and the shortage in alkaline activator, and thereby yielding geopolymers with relatively poor mechanical strength (Fig. 3a vs 3b). However, the introduction of waterglass appears to facilitate the

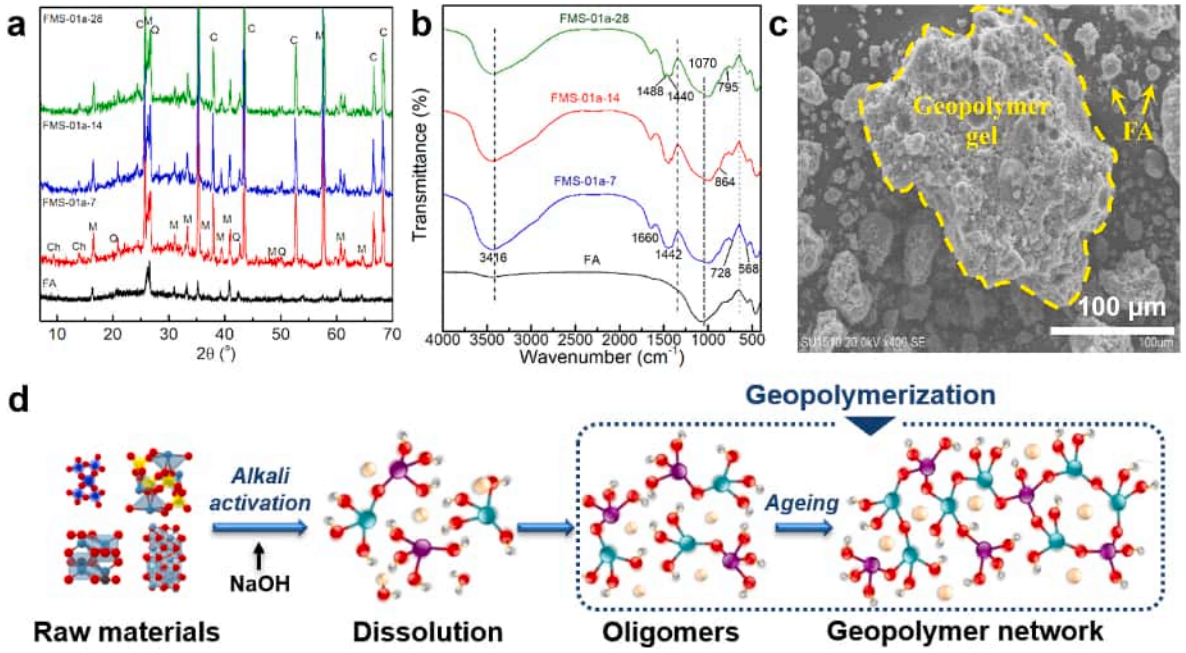

Fig. 5. (**a**) XRD patterns (Note: C= Corundum, Ch = Chabazite, M = Mullite, Q = Quartz), (**b**) FTIR spectra of geopolymers activated by 10 M NaOH and cured for varying days (i.e., FMS-a series); (**c**) SEM image of specimen cured for 14 days, (**d**) the proposed geopolymerization procedure of the mixture of MT and FA by NaOH solution (Note: Si, purple ball; Al, cyan ball; Na, wheat ball; S, yellow ball; O, red ball; H, grey ball.).

formation of geopolymer gel particularly in the matrix with 100 % of FA (Fig. S9), demonstrating that the addition of waterglass can notably change their microstructural properties and thereby improving their compressive strength accordingly (see Fig. 4d−f). Additionally, incorporating 5 wt% of Gp was found to facilitate the formation of both calcite (JCPDS #05–0586) and calcium silicate (JCPDS #31–0302, Fig. S10), both of which are beneficial for the early strength of the resulting geopolymers (Li et al., 2016b; Luukkonen et al., 2018). The integrating of Ca2+ from Gp in the bond Si–O–Al–O can not only equilibrate the charged Al3+ ions but also contribute strongly to the formation of C–S–H gel (Fig. S10h), therefore leading to the improvement of compressive strength (Fig. 4g−i).

However, further increasing the dosage of Gp up to 10 wt% appears to result in inadequate geopolymerization reactions, thus leaving a large amount of unreacted FA and Gp in the geopolymer specimens (Fig. S11). Cointegrating of Gp and waterglass into the geopolymer matrixes seems not to alter their microstructural properties too much (Figs. S12–13) as compared to those with 10 wt% Gp and activated with 5 M NaOH (Fig. S11). Although the early microstructure of the resulting geopolymer appears to be improved by replacing 5 M with 10 M NaOH to activate the above matrixes (Fig. S14 vs S13), after curing for 28 days, however, the large geopolymer gels found in the early samples (Fig. S14h) were fragmented due to the conversion of amorphous gels to crystalline minerals over time (Fig. S14), thereby reducing their compressive strength. Crystallization of such amorphous gels into zeolites (e.g., chabazite (JCPDS #52–0784) in Fig. S14b) may somewhat enhance their sequestration for hazardous elements (Bah et al., 2022b), but at the expense of their mechanical strength and long-term durability.

Nevertheless, to increase the feasibility of the alkali-activated geopolymerization technique and reduce its cost and environmental impact, further considerations are needed, including the possibility of improving the strength and long-term durability of geopolymer products by curing at elevated temperatures (Bah et al., 2022a), and substituting sodium hydroxide with industrial alkaline waste (Ouffa et al., 2022).

4. Conclusions

Geopolymerization was applied to valorize the lead-zinc mine tailings with the blending of class F fly ash and flue gas desulfurization (FGD) gypsum in this study. The results of visual inspection and mechanical strength testing revealed that the dimensional stability and the unconfined compressive strength (UCS) of geopolymers are dependent on sodium hydroxide (NaOH) molarity, dosages of fly ash, gypsum, and waterglass, as well as the curing time. The geopolymer matrixes with 100 wt% of fly ash and activated by 10 M NaOH were found to demonstrate the highest UCS. With the blending of increasing amounts of mine tailing, the compressive strength decreased accordingly due to the less amount of active alumina and silica in mine tailing compared to fly ash. The incorporation of 5 wt% gypsum would lead to strength improvement, particularly for matrixes with 50–75 wt% fly ash. The introduction of 12.5 wt% waterglass can also facilitate the geopolymerization and thus increase the strength of the resulting matrixes. Cointegrating of gypsum and waterglass into the geopolymer matrixes, however, would induce antagonistic effects on both the dimensional stability and the strength development. Microstructural analysis indicated that the strength of the fly ash/mine tailing-based geopolymer is mainly contributed by dense amorphous gels, which were converted to crystalline minerals gradually over time, leading to a decrease in strength. This study demonstrated that lead-zinc mine tailings could be successfully valorized through geopolymerization for yielding products with potential applications in the construction industry. To increase the feasibility and lower the environmental impact of this geopolymerization technique, further considerations such as heat-curing and using industrial alkaline waste are needed.

CRediT authorship contribution statement

Dawei Li: Investigation. **Andrea O. Ramos:** Methodology, Visualization, Investigation, Writing – original draft. **Alseny Bah:** Visualization, Investigation, Writing – original draft. **Feihu Li:** Conceptualization, Visualization, Methodology, Writing – original draft, Writing – review & editing, Supervision.

Declaration of competing interest

The authors declare that they have no known competing financial interests or personal relationships that could have appeared to influence the work reported in this paper.

Data availability

Data will be made available on request.

Acknowledgments

This work is partially supported by NFSC (52000101). The authors are thankful to Jiangsu Nanre Power Generation Co., Ltd. (Nanjing, China) and Nanjing Yinmao Pb–Zn Mining Industry Co., Ltd. (Nanjing, China) for providing raw materials, and to Dr. Fengying Li for the access to portable XRF apparatus.

Appendix A. Supplementary data

Supplementary data to this article can be found online at https://doi.org/10.1016/j.jenvman.2023.119501.

References

Ahmari, S., Zhang, L.Y., 2013. Utilization of cement kiln dust (CKD) to enhance mine tailings-based geopolymer bricks. Construct. Build. Mater. 40, 1002–1011. https://doi.org/10.1016/j.conbuildmat.2012.11.069.

Alvarez-Ayuso, E., 2022. Stabilization and encapsulation of arsenic-/antimony-bearing mine waste: overview and outlook of existing techniques. Crit. Rev. Environ. Sci. Technol. 52 (20), 3720–3752. https://doi.org/10.1080/10643389.2021.1944588.

Aouan, B., Alehyen, S., Fadil, M., El Alouani, M., Saufi, H., El Herradi, E.H., El Makhoukhi, F., Taibi, M.h., 2023. Development and optimization of geopolymer adsorbent for water treatment: application of mixture design approach. J. Environ. Manag. 338, 117853 https://doi.org/10.1016/j.jenvman.2023.117853.

ASTM Standard C109/C109M-08, 2009. Standard Test Method for Compressive Strength of Hydraulic Cement Mortars (Using 2-in. Or [50-mm] Cube Specimens). ASTM International, West Conshohocken, PA, USA. https://doi.org/10.1520/C0109_C0109M-08.

Bah, A., Feng, D.L., Kedjanyi, E.A.K., Shen, Z.Y., Bah, A., Li, F.H., 2022a. Solidification of (Pb-Zn) mine tailings by fly ash-based geopolymer I: influence of alkali reagents ratio and curing condition on compressive strength. J. Mater. Cycles Waste Manag. 24 (1), 351–363. https://doi.org/10.1007/s10163-021-01322-4.

Bah, A., Jin, J., Ramos, A.O., Bao, Y., Ma, M.Y., Li, F.H., 2022b. Arsenic(V) immobilization in fly ash and mine tailing-based geopolymers: performance and mechanism insight. Chemosphere 306, 135636. https://doi.org/10.1016/j.chemosphere.2022.135636.

Behera, S.K., Ghosh, C.N., Mishra, K., Mishra, D.P., Singh, P., Mandal, P.K., Buragohain, J., Sethi, M.K., 2020. Utilisation of lead-zinc mill tailings and slag as paste backfill materials. Environ. Earth Sci. 79 (16), 389. https://doi.org/10.1007/s12665-020-09132-x.

Boonserm, K., Sata, V., Pimraksa, K., Chindaprasirt, P., 2012. Improved geopolymerization of bottom ash by incorporating fly ash and using waste gypsum as additive. Cem. Concr. Compos. 34 (7), 819–824. https://doi.org/10.1016/j.cemconcomp.2012.04.001.

Choi, W.H., Lee, S.R., Park, J.Y., 2009. Cement based solidification/stabilization of arsenic-contaminated mine tailings. Waste Manag. (Tucson, Ariz.) 29 (5), 1766–1771. https://doi.org/10.1016/j.wasman.2008.11.008.

Dadsetan, S., Siad, H., Lachemi, M., Sahmaran, M., 2021. Evaluation of the tridymite formation as a technique for enhancing geopolymer binders based on glass waste. J. Clean. Prod. 278, 123983 https://doi.org/10.1016/j.jclepro.2020.123983.

Duxson, P., Fernandez-Jimenez, A., Provis, J.L., Lukey, G.C., Palomo, A., van Deventer, J. S.J., 2007. Geopolymer technology: the current state of the art. J. Mater. Sci. 42 (9), 2917–2933. https://doi.org/10.1007/s10853-006-0637-z.

Fernandez-Jimenez, A., Garcia-Lodeiro, I., Palomo, A., 2007. Durability of alkali-activated fly ash cementitious materials. J. Mater. Sci. 42 (9), 3055–3065. https://doi.org/10.1007/s10853-006-0584-8.

He, X., Yuhua, Z.H., Qaidi, S., Isleem, H.F., Zaid, O., Althoey, F., Ahmad, J., 2022. Mine tailings-based geopolymers: a comprehensive review. Ceram. Int. 48 (17), 24192–24212. https://doi.org/10.1016/j.ceramint.2022.05.345.

Jiang, G.H., Min, X.B., Ke, Y., Liang, Y.J., Yan, X., Xu, W.B., Lin, Z., 2022. Solidification/stabilization of highly toxic arsenic-alkali residue by MSWI fly ash-based cementitious material containing Friedel's salt: efficiency and mechanism. J. Hazard Mater. 425, 127992 https://doi.org/10.1016/j.jhazmat.2021.127992.

Jiang, H.Q., Qi, Z.J., Yilmaz, E., Han, J., Qiu, J.P., Dong, C.L., 2019. Effectiveness of alkali-activated slag as alternative binder on workability and early age compressive strength of cemented paste backfills. Construct. Build. Mater. 218, 689–700. https://doi.org/10.1016/j.conbuildmat.2019.05.162.

Ken, P.W., Ramli, M., Ban, C.C., 2015. An overview on the influence of various factors on the properties of geopolymer concrete derived from industrial by-products. Construct. Build. Mater. 77, 370–395. https://doi.org/10.1016/j.conbuildmat.2014.12.065.

Khale, D., Chaudhary, R., 2007. Mechanism of geopolymerization and factors influencing its development: a review. J. Mater. Sci. 42 (3), 729–746. https://doi.org/10.1007/s10853-006-0401-4.

Kiventera, J., Sreenivasan, H., Cheeseman, C., Kinnunen, P., Illikainen, M., 2018. Immobilization of sulfates and heavy metals in gold mine tailings by sodium silicate and hydrated lime. J. Environ. Chem. Eng. 6 (5), 6530–6536. https://doi.org/10.1016/j.jece.2018.10.012.

Krishna, R.S., Shaikh, F., Mishra, J., Lazorenko, G., Kasprzhitskii, A., 2021. Mine tailings-based geopolymers: properties, applications and industrial prospects. Ceram. Int. 47 (13), 17826–17843. https://doi.org/10.1016/j.ceramint.2021.03.180.

Lazorenko, G., Kasprzhitskii, A., Shaikh, F., Krishna, R.S., Mishra, J., 2021. Utilization potential of mine tailings in geopolymers: physicochemical and environmental aspects. Process Saf. Environ. Protect. 147, 559–577. https://doi.org/10.1016/j.psep.2020.12.028.

Li, F.H., Li, Q., Zhai, J.P., Sheng, G.H., 2007. Effect of zeolitization of CFBC fly ash on immobilization of Cu2+, Pb2+, and Cr3+. Ind. Eng. Chem. Res. 46 (22), 7087–7095. https://doi.org/10.1021/ie070218v.

Li, F.H., Wu, W.H., Li, R.Y., Fu, X.R., 2016a. Adsorption of phosphate by acid-modified fly ash and palygorskite in aqueous solution: experimental and modeling. Appl. Clay Sci. 132, 343–352. https://doi.org/10.1016/j.clay.2016.06.028.

Li, Q., Xu, H., Li, F.H., Li, P.M., Shen, L.F., Zhai, J.P., 2012. Synthesis of geopolymer composites from blends of CFBC fly and bottom ashes. Fuel 97, 366–372. https://doi.org/10.1016/j.fuel.2012.02.059.

Li, Y.C., Min, X.B., Chai, L.Y., Shi, M.Q., Tang, C.J., Wang, Q.W., Liang, Y.J., Lei, J., Liyang, W.J., 2016b. Co-treatment of gypsum sludge and Pb/Zn smelting slag for the solidification of sludge containing arsenic and heavy metals. J. Environ. Manag. 181, 756–761. https://doi.org/10.1016/j.jenvman.2016.07.031.

Luukkonen, T., Abdollahnejad, Z., Yliniemi, J., Kinnunen, P., Illikainen, M., 2018. One-part alkali-activated materials: a review. Cement Concr. Res. 103, 21–34. https://doi.org/10.1016/j.cemconres.2017.10.001.

Mabroum, S., Aboulayt, A., Taha, Y., Benzaazoua, M., Semlal, N., Hakkou, R., 2020. Elaboration of geopolymers based on clays by-products from phosphate mines for construction applications. J. Clean. Prod. 261, 121317 https://doi.org/10.1016/j.jclepro.2020.121317.

Majidi, B., 2009. Geopolymer technology, from fundamentals to advanced applications: a review. Mater. Technol. 24 (2), 79–87. https://doi.org/10.1179/175355509x449355.

Malviya, R., Chaudhary, R., 2006. Factors affecting hazardous waste solidification/stabilization: a review. J. Hazard Mater. 137 (1), 267–276. https://doi.org/10.1016/j.jhazmat.2006.01.065.

Manjarrez, L., Nikvar-Hassani, A., Shadnia, R., Zhang, L.Y., 2019. Experimental study of geopolymer binder synthesized with copper mine tailings and low-calcium copper slag. J. Mater. Civ. Eng. 31 (8), 04019156 https://doi.org/10.1061/(Asce)Mt.1943-5533.0002808.

Manjarrez, L., Zhang, L.Y., 2018. Utilization of copper mine tailings as road base construction material through geopolymerization. J. Mater. Civ. Eng. 30 (9), 04018201 https://doi.org/10.1061/(Asce)Mt.1943-5533.0002397.

Mohajerani, A., Suter, D., Jeffrey-Bailey, T., Song, T.Y., Arulrajah, A., Horpibulsuk, S., Law, D., 2019. Recycling waste materials in geopolymer concrete. Clean Technol. Environ. Policy 21 (3), 493–515. https://doi.org/10.1007/s10098-018-01660-2.

Nguyen, H.-H.T., Nguyen, H.T., Ahmed, S.F., Rajamohan, N., Yusuf, M., Sharma, A., Arunkumar, P., Deepanraj, B., Tran, H.-T., Al-Gheethi, A., Vo, D.-V.N., 2023. Emerging waste-to-wealth applications of fly ash for environmental remediation: a review. Environ. Res. 227, 115800 https://doi.org/10.1016/j.envres.2023.115800.

Oh, J.E., Monteiro, P.J.M., Jun, S.S., Choi, S., Clark, S.M., 2010. The evolution of strength and crystalline phases for alkali-activated ground blast furnace slag and fly ash-based geopolymers. Cement Concr. Res. 40 (2), 189–196. https://doi.org/10.1016/j.cemconres.2009.10.010.

Olympus, 2013. DELTA Family Handheld XRF Analyzer: User's Manual, International ed. Waltham, MA, USA.

Opiso, E.M., Tabelin, C.B., Maestre, C.V., Aseniero, J.P.J., Park, I., Villacorte-Tabelin, M., 2021. Synthesis and characterization of coal fly ash and palm oil fuel ash modified artisanal and small-scale gold mine (ASGM) tailings based geopolymer using sugar mill lime sludge as Ca-based activator. Heliyon 7 (4), e06654. https://doi.org/10.1016/j.heliyon.2021.e06654.

Ouffa, N., Trauchessec, R., Benzaazoua, M., Lecomte, A., Belem, T., 2022. A methodological approach applied to elaborate alkali-activated binders for mine paste backfills. Cem. Concr. Compos. 127, 104381 https://doi.org/10.1016/j.cemconcomp.2021.104381.

Park, I., Tabelin, C.B., Jeon, S., Li, X.L., Seno, K., Ito, M., Hiroyoshi, N., 2019. A review of recent strategies for acid mine drainage prevention and mine tailings recycling. Chemosphere 219, 588–606. https://doi.org/10.1016/j.chemosphere.2018.11.053.

Prasad, P.S.R., 2005. Direct formation of the γ-CaSO4 phase in dehydration process of gypsum: in situ FTIR study. Am. Mineral. 90 (4), 672–678. https://doi.org/10.2138/am.2005.1742.

Provis, J.L., Bernal, S.A., 2014. Geopolymers and related alkali-activated materials. Annu. Rev. Mater. Res. 44, 299–327. https://doi.org/10.1146/annurev-matsci-070813-113515.

Provis, J.L., Yong, C.Z., Duxson, P., van Deventer, J.S.J., 2009. Correlating mechanical and thermal properties of sodium silicate-fly ash geopolymers. Colloids Surf., A 336 (1–3), 57–63. https://doi.org/10.1016/j.colsurfa.2008.11.019.

Rao, F., Liu, Q., 2015. Geopolymerization and its potential application in mine tailings consolidation: a review. Miner. Process. Extr. Metall. Rev. 36 (6), 399–409. https://doi.org/10.1080/08827508.2015.1055625.

Rees, C.A., Provis, J.L., Lukey, G.C., van Deventer, J.S.J., 2007. In situ ATR-FTIR study of the early stages of fly ash geopolymer gel formation. Langmuir 23 (17), 9076–9082. https://doi.org/10.1021/la701185g.

Ren, X., Zhang, L.Y., Ramey, D., Waterman, B., Ormsby, S., 2015. Utilization of aluminum sludge (AS) to enhance mine tailings-based geopolymer. J. Mater. Sci. 50 (3), 1370–1381. https://doi.org/10.1007/s10853-014-8697-y.

Sheng, G.H., Zhai, J.P., Li, Q., Li, F.H., 2007. Utilization of fly ash coming from a CFBC boiler co-firing coal and petroleum coke in Portland cement. Fuel 86 (16), 2625–2631. https://doi.org/10.1016/j.fuel.2007.02.018.

Shi, C.J., Qu, B., Provis, J.L., 2019. Recent progress in low-carbon binders. Cement Concr. Res. 122, 227–250. https://doi.org/10.1016/j.cemconres.2019.05.009.

Singh, J., Singh, S.P., 2019. Geopolymerization of solid waste of non-ferrous metallurgy - a review. J. Environ. Manag. 251, 109571 https://doi.org/10.1016/j.jenvman.2019.109571.

Wang, S.Y., Liu, B., Zhang, Q., Wen, Q., Lu, X.H., Xiao, K., Ekberg, C., Zhang, S.E., 2023. Application of geopolymers for treatment of industrial solid waste containing heavy metals: state-of-the-art review. J. Clean. Prod. 390, 136053 https://doi.org/10.1016/j.jclepro.2023.136053.

Xia, M., Muhammad, F., Zeng, L.H., Li, S., Huang, X., Jiao, B.Q., Shiau, Y., Li, D.W., 2019. Solidification/stabilization of lead-zinc smelting slag in composite based geopolymer. J. Clean. Prod. 209, 1206–1215. https://doi.org/10.1016/j.jclepro.2018.10.265.

Zhang, J., Shi, C.J., Zhang, Z.H., Ou, Z.H., 2017. Durability of alkali-activated materials in aggressive environments: a review on recent studies. Construct. Build. Mater. 152, 598–613. https://doi.org/10.1016/j.conbuildmat.2017.07.027.

Zhang, L.Y., Ahmari, S., Zhang, J.H., 2011. Synthesis and characterization of fly ash modified mine tailings-based geopolymers. Construct. Build. Mater. 25 (9), 3773–3781. https://doi.org/10.1016/j.conbuildmat.2011.04.005.

Zhang, N., Hedayat, A., Perera-Mercado, Y., Sosa, H.G.B., Tupa, N., Morales, I.Y., Loza, R.S.C., 2022. Including class F fly ash to improve the geopolymerization effects and the compressive strength of mine tailings-based geopolymer. J. Mater. Civ. Eng. 34 (11), 04022313 https://doi.org/10.1061/(Asce)Mt.1943-5533.0004465.

Zhang, N., Hedayat, A., Sosa, H.G.B., Bernal, R.P.H., Tupa, N., Morales, I.Y., Loza, R.S.C., 2021a. On the incorporation of class F fly-ash to enhance the geopolymerization effects and splitting tensile strength of the gold mine tailings-based geopolymer. Construct. Build. Mater. 308, 125112 https://doi.org/10.1016/j.conbuildmat.2021.125112.

Zhang, N., Hedayat, A., Sosa, H.G.B., Cardenas, J.J.G., Alvarez, G.E.S., Rivera, V.B.A., 2021b. Damage evaluation and deformation behavior of mine tailing-based Geopolymer under uniaxial cyclic compression. Ceram. Int. 47 (8), 10773–10785. https://doi.org/10.1016/j.ceramint.2020.12.194.

Zhang, P.P., Muhammada, F., Yu, L., Xia, M., Lin, H.R., Huang, X., Jiao, B.Q., Shiau, Y.C., Li, D.W., 2020. Self-cementation solidification of heavy metals in lead-zinc smelting slag through alkali-activated materials. Construct. Build. Mater. 249, 118756 https://doi.org/10.1016/j.conbuildmat.2020.118756.

Zhang, X.L., Zhang, S.Y., Hui, L., Zhao, Y.L., 2021c. Disposal of mine tailings via geopolymerization. J. Clean. Prod. 284, 124756 https://doi.org/10.1016/j.jclepro.2020.124756.